Naval Research Laboratory
Washington, DC 20375-5320

NRL/5620/MR—2021/1

Homogeneity Characterization of Photonic Crystal Fiber

RAFAEL GATTASS

L. BRANDON SHAW

DANIEL RHONEHOUSE

SHYAM BAYYA

JASBINDER S. SANGHERA

Optical Materials and Devices Branch
Optical Sciences Division

August 26, 2021

REPORT DOCUMENTATION PAGE

Form Approved
OMB No. 0704-0188

1. REPORT DATE *(DD-MM-YYYY)*
26-08-2021

2. REPORT TYPE
NRL Memorandum Report

3. DATES COVERED *(From - To)*
10/01/2020 – 9/30/2021

4. TITLE AND SUBTITLE
Homogeneity characterization of Photonic Crystal Fiber

5a. CONTRACT NUMBER

5b. GRANT NUMBER

5c. PROGRAM ELEMENT NUMBER
62114N

6. AUTHOR(S)
Rafael R. Gattass, L. Brandon Shaw, Daniel Rhonehouse, Shyam Bayya, and Jasbinder S. Sanghera

5d. PROJECT NUMBER

5e. TASK NUMBER

5f. WORK UNIT NUMBER
6B70

7. PERFORMING ORGANIZATION NAME(S) AND ADDRESS(ES)
Naval Research Laboratory
4555 Overlook Avenue, SW
Washington, DC 20375-5320

8. PERFORMING ORGANIZATION REPORT NUMBER
NRL/5620/MR--2021/1

9. SPONSORING / MONITORING AGENCY NAME(S) AND ADDRESS(ES)
Naval Research Laboratory
4555 Overlook Avenue, SW
Washington, DC 20375-5320

10. SPONSOR / MONITOR'S ACRONYM(S)

11. SPONSOR / MONITOR'S REPORT NUMBER(S)

12. DISTRIBUTION / AVAILABILITY STATEMENT
DISTRIBUTION STATEMENT A: Approved for public release; distribution is unlimited.

13. SUPPLEMENTARY NOTES

14. ABSTRACT
We demonstrate the use of spontaneous four- wave mixing (FWM) as a method to determine the homogeneity of photonic crystal fibers. Two fibers are drawn under different conditions and characterized optically. The optical cross sections of the fibers are modeled in a full vectorial finite element analysis software to determine the effective propagations constants. The modeled propagation constants can be used to calculate the four- wave mixing wavelength peak and compared to the measured value. Given the resolution of the features inside photonic crystal fibers, measuring the four- wave mixing peak wavelength serves as a direct measure on the homogeneity of the fiber, in particular the key metric used was the spatial variation of the four-wave mixing wavelength along the length of the fiber. This report presents research conducted by Optical Sciences code 5600 for the development of high power fiber laser sources based on four-wave mixing.

15. SUBJECT TERMS
Fiber lasers — Four wave mixing
Photonic crystal fiber — Frequency conversion

16. SECURITY CLASSIFICATION OF: a. REPORT	b. ABSTRACT	c. THIS PAGE	17. LIMITATION OF ABSTRACT	18. NUMBER OF PAGES	19a. NAME OF RESPONSIBLE PERSON
U	U	U	U	10	Rafael Gattass
					19b. TELEPHONE NUMBER *(include area code)* (202) 404-5459

Standard Form 298 (Rev. 8-98)
Prescribed by ANSI Std. Z39.18

This page intentionally left blank.

CONTENTS

This page intentionally left blank.

EXECUTIVE SUMMARY

We demonstrate the use of spontaneous four wave mixing as a method to determine the homogeneity of photonic crystal fibers. Two fibers are drawn under different conditions and characterized optically. The optical cross sections of the fibers are modeled in a full vectorial finite element analysis software to determine the effective propagations constants. The modeled propagation constants can be used to calculate the four wave mixing wavelength peak and compared to the measured value. Given the resolution of the features inside photonic crystal fibers, measuring the four wave mixing peak wavelength serves as a direct measure on the homogeneity of the fiber, in particular the key metric used was the spatial variation of the four-wave mixing wavelength along the length of the fiber.

This report presents research conducted by Optical Sciences code 5600 for the development of high power fiber laser sources based on four-wave mixing.

This page intentionally left blank.

HOMOGENEITY CHARACTERIZATION OF PHOTONIC CRYSTAL FIBERS

1. INTRODUCTION

Four wave mixing is a nonlinear process that allows for efficient conversion of pump light to two separate wavelength, one shorter than the pump typically called signal and a longer wavelength typically called idler. This process can be quite efficient [1,2], and there have been a few demonstrations of watt level FWM conversion to the visible. [3-6]. FWM, like most nonlinear processes, depends on the careful phase matching between propagating wavelengths to be efficient. In a fiber, the longer this phase matching may be maintained the higher the expected efficiency of the process. However, most demonstrations so far have been restricted to short fibers < 3 m and the use of high peak power sources to enable efficient four wave mixing. One possible reason is the lack of homogeneity in the fibers used, leading to large variations on the phase matching process over lengths exceeding 1 m.

In the most recent FWM demonstrations, photonic crystal fibers (PCF) are used to convert 1 um light to the visible and SWIR range. [3-6] Photonic crystal fibers display all the advantages of a core-clad fiber for FWM conversion such as high coupling of light from the fiber pump source, long interaction length, and inherent control over the modal overlap. However, they also enable enormous control over the dispersion profile of the fiber and hence the phase-matching between waves. The most commonly fabricated PCF is based on a hexagonal pattern of air holes. The PCF propagation characteristics can be determined solely by the pitch of the hexagonal holes as well as the hole diameters along the fiber cross section. Control over the pitch and the hole diameter along the fiber however is not the subject of active research and depending on the fiber design, the optical properties can be quite sensitive to small variations on the hole diameter. [7-9]

In this report we describe our methods and results for determining the variation of a series of photonic crystal fibers fabricated at Optical Sciences Division of US Naval Research Laboratory. We have been working on several methods to improve the homogeneity of PCFs. Although we can characterize the outer diameter variation easily, determining the impact of our improvements on the stability of the pitch or the homogeneity of the air holes remains quite challenging. This challenge is compounded by the dimensions of the holes variations (typically in the sub-micrometer range) as well as need for timely feedback when performing research on fiber draw. Our goal is identify a method to quickly characterize the impact of the fabrication improvements in on new fibers. We demonstrate that measuring the FWM wavelength in short pieces of fibers serves as a good metric to characterize the homogeneity of the fabricated fibers.

2. APPROACH

2.1 Modeling Dispersion

To determine the dispersion of the photonic crystal fiber fabricated, full vector finite element modeling was performed through a commercial software (COMSOL) to model the supported modes of the fiber and their propagation constants (effective index). The mode solver is parametrically sweep with respect to the propagation wavelength, yielding a map of effective indexes versus wavelength. This data is then processed to determine the dispersion of the fiber. The dispersion of each fiber can then be used to determine the expected four-wave mixing wavelength for a given pump power.

Each fiber section was cleaved using an ultrasonic fiber cleaver (FK-11 York) or with a blade cleaver depending on the fiber dimensions. A high resolution image of the end face of the fiber was captured with a confocal microscope. Each image is further processed by converting the image into a binary image and fitting the holes of the binary image to a series of ellipses. Each ellipse position, major axis, minor axis and angle is exported and a model image is formed for COMSOL. A sample image of the original fiber and the binary fiber end face is shown in Figure 1a and 1b.

Manuscript approved August 9, 2021.

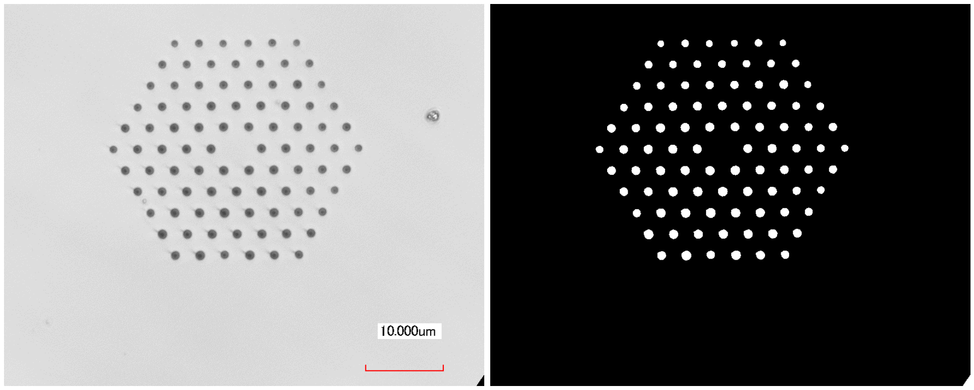

(a) (b)

Fig. 1 — (a) Sample PCF cross section confocal image. (b) Black and white (binary) conversion of the image in (a).

To ensure the convergence of the model, a perfectly electric boundary condition is imposed around the holes. Placement of the boundary condition close to the last array of hole is crucial to ensure the solved modes are the ones propagating inside the core.

2.2 Measuring FWM wavelength

A direct measurement of the dispersion of the fiber is a complex measurement for short fibers (< 1m). Although there are ways to perform this measurement (pulse/spectral broadening or white light interferometry for example), the key parameter we are attempting to control is the four-wave mixing efficiency. Therefore we decide to measure the FWM wavelength directly for several sections of the same optical fiber. Although this process is destructive in nature, it did allow for spatial sectioning could on a 0.5 m scale and measurements could be accomplished on a reasonable time scale.

A microchip laser operating at 1064 nm with pulse width of 800 ps and variable pulse repetition rate from 10 kHz to 100 kHz was used as the pump source for these fibers. The microchip was capable of reaching up to 100 kW of peak power, well beyond the expected threshold of 1 - 10 kW. The microchip was surprisingly sensitive to back reflections so a fiber isolator was added to the setup to avoid back reflections. Figure 2 shows a schematic of the setup and an image of the setup in the laboratory. A 30 mm lens was used to couple the laser beam into the fiber.

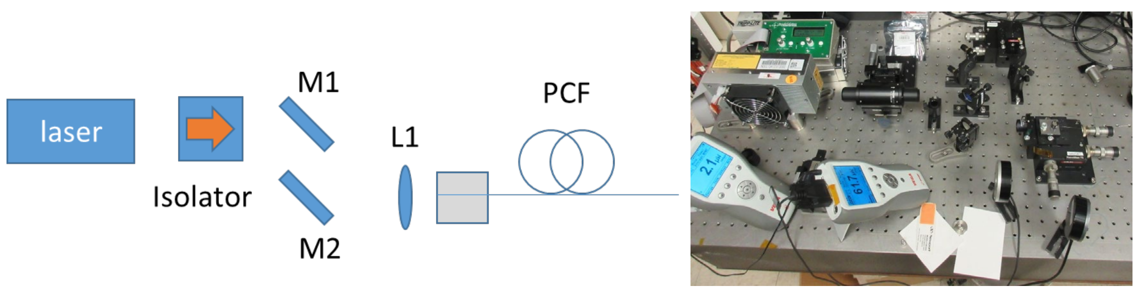

(a) (b)

Fig. 2 — (a) Schematic of laser test bed. Laser: Wedge HF 1064, Isolator: Thorlabs IO-8-1064, M1 and M2 Thorlabs broadband dielectric mirrors, L1: 1064 nm Achromatic lens focal length 30 mm, (b) Image of test bed in lab.

3. EXPERIMENTS

To validate the concept of monitoring homogeneity through the four wave mixing peak in short pieces of fibers two distinct photonic crystal fiber draw conditions were used. In the first case, "typical" fiber draw conditions were used and a fiber design with high nonlinearity and normal dispersion at the pump wavelength of 1064 was targeted. The second case, used a high-stability drawing condition where a longer lag time was provided for the fiber draw to start, increasing the thermal stability, which let to fiber draw lengths are reduced slightly (100s of meters). The fiber design was also adjusted to sacrificing some of the nonlinearity but reducing the requirements on pressure regularization. For both cases, over 100 m of each fiber was fabricated, allowing us to characterize different sections of the fiber and determine the stability along the length.

3.1 Results for PCF1: typical fiber draw

PCF1 was assembled by stack and draw of high purity silica capillaries with a hexagonal PCF design target having 3.2 µm pitch (Λ) and 0.98 µm hole diameter (d), for hole diameter to pitch ratio of 0.35. The stacked preform is drawn down into a cane and drawn at the fiber draw tower. The fabricated fiber deviated slightly from the target design, displaying at pitch of 3.15 µm and a hole diameter of 1.09 µm for a d/Λ ratio of 0.35. These fibers were drawn under high tension and high speed. The fiber outer diameter was measured to be 150 µm, with a measured 2.2 µm fluctuation over a 60 m length, a variation on the order of those typically for commercial PCFs.

The long piece of fiber was cut into sub sections spanning 5 m, 10 m and 15 m. The cross section of the end faces of each section was imaged with the confocal microscope. The fiber displayed small variations in the hole diameter along the cross section. However, on average no measurable variation in the difference between hole diameters could be detected (the resolution of the confocal microscope is 170 nm).

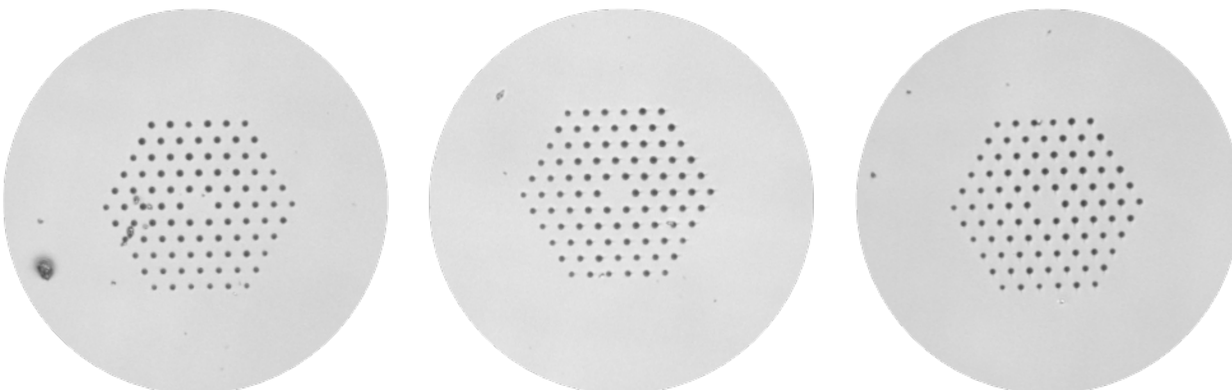

(a) (b) (c)

Fig. 3 — (a) Confocal images of sections of PCF draw. The dimensions of the pitch remained constant for all three draws at 3.08 µm, while the average hole diameter varies from 1.06, 1.08 and 1.05 µm.

Each subsection was cut down further, removing ~ 1.5 m pieces from the beginning and the end of each fiber. We were unable to determine meaningful differences on the average fiber parameters from the imaging of these smaller subsections. Each subsection was tested with the pulsed laser to determine the spontaneous FWM peak wavelength. Figure 4 shows the variation of the FWM wavelength along different lengths of fiber for three sections of the fiber draw. As can be seen visually, the FWM generated wavelength varies both from overall section to section but also with a single piece (either 5m, 10m or 15m). The average measured variation of the FWM peak is 3.6 ± 0.2 nm per 10 m section.

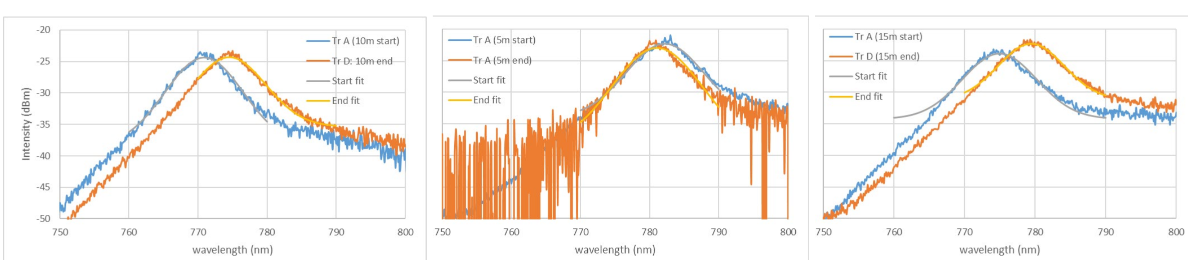

(a) (b) (c)

Fig. 4 — (a) Confocal image of the "low" tension PCF, (b) modeled mode field diameter at 1050 nm, (c) signal and idler wavelengths as a function of pump wavelength calculated from the modeled effective indexes.

3.2 Results for PCF2: high stability draw

PCF2 was also assembled through stack and draw. The hexagonal fiber design was adjusted slightly with the pitch being 4.2 µm and hole diameter set to 1.47 µm, providing a hole diameter to pitch ratio of 0.35. The new preform used a different set of capillaries and allowed for the preform to be much closer to the expected pitch and hole diameter than the previous version. This reduced the required pressure needed to be applied to the holes. However, the final fiber displayed at pitch of 4.11 µm and a hole diameter of 1.88 +- 0.06 µm. Highlighting the higher stability of this draw, the fiber had an outer diameter of 200 µm but only displayed a diameter fluctuation of 0.3 µm over a 17 m length.

Similar to the work performed on PCF1, a large 10 m long piece of fiber was sectioned in different parts with each section characterized. Figure 4 shows a confocal image of the fiber cross-section, a sample supported optical mode determined by the COMSOL simulation and the FWM matching wavelengths (based on the simulated effective indexes). . One can easily see that the holes are much larger in this fiber, and that the hole diameter fluctuation across the cross-section was much smaller than the previous fiber.

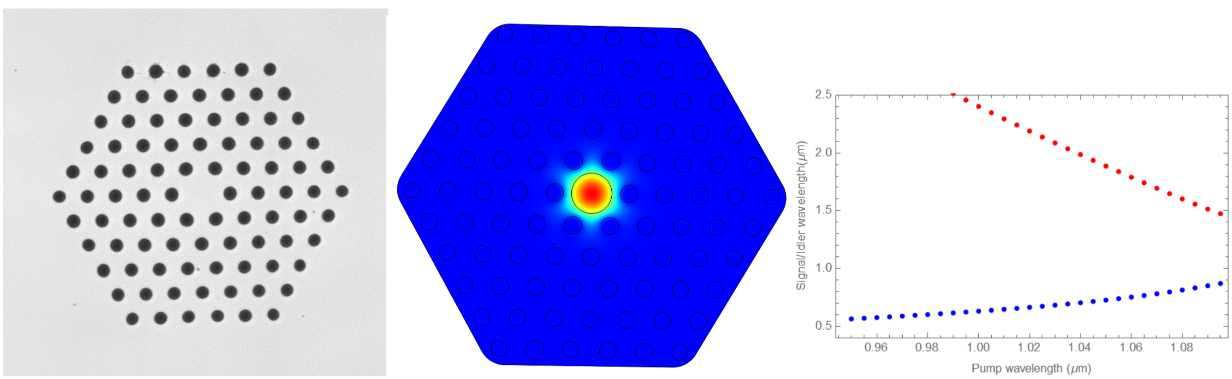

(a) (b) (c)

Fig. 4 — (a) Confocal image of the “high” tension PCF, (b) modeled mode field diameter at 1050 nm, (c) signal and idler wavelengths as a function of pump wavelength calculated from the modeled effective indexes.

The fiber was tested with the microchip laser in the same manner as the previous fiber and the measured spectrum for the fiber is shown in Figure 5. The peak wavelength for the spontaneous FWM spectrum was fitted to a Gaussian and the center wavelengths were determined to be 763.5 nm and 763.7 nm with a peak estimate error of 0.2 nm.

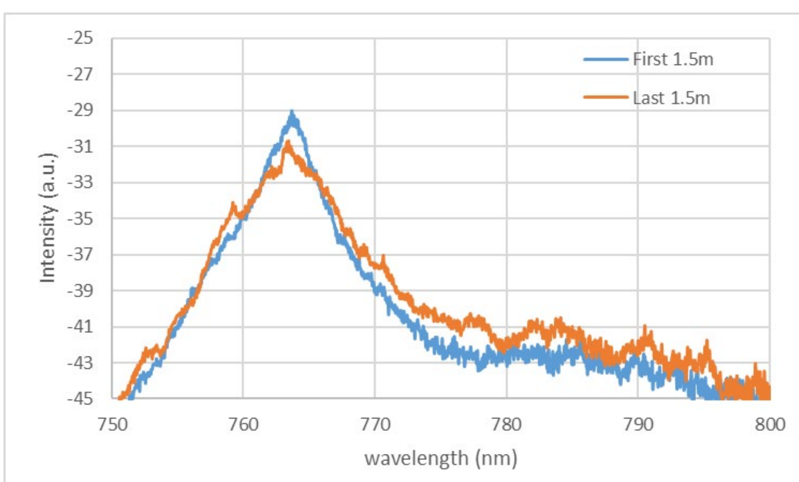

Fig. 5 — FWM spectrum output from first 1.5m of 10 m piece (blue) and last 1.5m (orange).

The high-stability fiber draw used in this current fiber is reflected clearly in the improved control over the measured FWM wavelength. The variation of the four-wave mixing wavelength was reduced from of 3.6 ± 0.2 nm per 10 m section to a measured variation of 0.2 ± 0.2 nm per 10 m, representing a 18X improvement in the quality of the fiber.

4. CONCLUSIONS

We demonstrate that a compact microchip based laser system can be used to characterize the homogeneity of the fiber. The variations in the hole diameter are too small to be properly resolved by confocal microscopy however their impact on the FWM wavelength is large enough to be easily discerned. This approach was validated through the comparison of two PCFs fabricated under different fiber draw conditions. The current fiber spatial resolution used at 1.5m, however preliminary work confirm we can observe spontaneous FWM peak for fibers as short as 30 cm. The use of higher wavelength resolution optical spectrum analyzers would allow us to further monitor the impact of future refinements on the fabrication methods by monitoring the spontaneous FWM wavelength generated.

REFERENCES

1. Chen, Yijiang. "Four-Wave Mixing in Optical Fibers: Exact Solution." Journal of the Optical Society of America B 6, no. 11 (November 1, 1989): 1986–93. https://doi.org/10.1364/JOSAB.6.001986.

2. Marhic, M. E., K. K. Y. Wong, M. C. Ho, and L. G. Kazovsky. "92% Pump Depletion in a Continuous-Wave One-Pump Fiber Optical Parametric Amplifier." Optics Letters 26, no. 9 (May 1, 2001): 620–22. https://doi.org/10.1364/OL.26.000620.

3. Wadsworth, W., N. Joly, J. Knight, T. Birks, F. Biancalana, and P. Russell. "Supercontinuum and Four-Wave Mixing with Q-Switched Pulses in Endlessly Single-Mode Photonic Crystal Fibres." Optics Express 12, no. 2 (January 26, 2004): 299–309. https://doi.org/10.1364/OPEX.12.000299.

4. Nodop, D., C. Jauregui, D. Schimpf, J. Limpert, and A. Tunnermann. "Efficient High-Power Generation of Visible and Mid-Infrared Light by Degenerate Four-Wave-Mixing in a Large-Mode-Area Photonic-Crystal Fiber." Optics Letters 34, no. 22 (November 15, 2009): 3499–3501. https://doi.org/10.1364/OL.34.003499.

5. Lavoute, Laure, Jonathan C. Knight, Pascal Dupriez, and William J. Wadsworth. "High Power Red and Near-IR Generation Using Four Wave Mixing in All Integrated Fibre Laser Systems." Optics Express 18, no. 15 (July 19, 2010): 16193–205.

6. Jauregui, Cesar, Alexander Steinmetz, Jens Limpert, and Andreas Tünnermann. "High-Power Efficient Generation of Visible and Mid-Infrared Radiation Exploiting Four-Wave-Mixing in Optical Fibers." Optics Express 20, no. 22 (October 22, 2012): 24957–65. https://doi.org/10.1364/OE.20.024957

7. Wong, G. K. L., A. Y. H. Chen, S. W. Ha, R. J. Kruhlak, S. G. Murdoch, R. Leonhardt, J. D. Harvey, and N. Y. Joly. "Characterization of Chromatic Dispersion in Photonic Crystal Fibers Using Scalar Modulation Instability." Optics Express 13, no. 21 (October 17, 2005): 8662–70. https://doi.org/10.1364/OPEX.13.008662.

8. Chen, J. S. Y., S. G. Murdoch, R. Leonhardt, and J. D. Harvey. "Effect of Dispersion Fluctuations on Widely Tunable Optical Parametric Amplification in Photonic Crystal Fibers." Optics Express 14, no. 20 (October 2, 2006): 9491–9501. https://doi.org/10.1364/OE.14.009491.

9. Holdynski, Zbyszek, Marek Napierala, Pawel Mergo, and Tomasz Nasilowski. "Experimental Investigation of Supercontinuum Generation in Photonic Crystal Fibers Pumped With Sub-Ns Pulses." Journal of Lightwave Technology 33, no. 10 (May 2015): 2106–10. https://doi.org/10.1109/JLT.2015.2398895